DOI: 10.11844/cjcb.2026.07.0003
中国细胞生物学学报 Chinese Journal of Cell Biology 2026, 48(7): 1776–1787 CSTR: 32200.14.cjcb.2026.07.0003

· 研究论文 ·

鱿鱼反射素蛋白RefA1持续表达引起MDCK细胞紧密连接与极性功能紊乱

胡碧茹# 宋俊祎#*
(国防科技大学理学院, 长沙 410073)

摘要 头足纲动物利用反射素蛋白在虹细胞中组装周期性膜结构, 形成可调控的结构色, 但其在细胞内的运输路径、空间组织及功能实现等机制仍不明确。前期研究发现, 通过大肠杆菌异源表达所获得的反射素蛋白A1(reflectin A1, RefA1)对磷脂膜具有高度亲和性, 而通过瞬时转染在HEK-293T细胞内表达的RefA1具有沿微管骨架定向运输的特性。为此, 该研究选用具有囊泡运输能力和细胞骨架可塑性的MDCK细胞系作为平台, 构建了稳定表达鱿鱼反射素蛋白RefA1的细胞模型, 旨在探究其胞内运输行为及对细胞结构的影响。结果发现, RefA1虽未实现预期的微管导向性质膜下富集, 却显著破坏了细胞的形态与极性: 表达RefA1的细胞面积减小、紧密连接解体, 并陷入“增殖–脱落”循环而无法形成完整单细胞层。转录组分析表明, RefA1通过抑制*CLDN4*、*CDH1*、*PARD6B*等极性决定因子的表达, 同时上调*MYLK2*、*ROCK1*等收缩调控基因的表达, 严重扰乱了与细胞连接及极性建成相关的分子网络。这些结果首次揭示了反射素蛋白不仅能与膜及细胞骨架互作, 更具有主动调控细胞极性建立过程的功能, 为理解头足纲动物光学结构的细胞学基础提供了新视角, 也为蛋白质介导的细胞形态工程与仿生材料设计提供了新线索。

关键词 反射素蛋白; MDCK细胞; 细胞极性; 紧密连接; 转录组分析

Constitutive Expression of Squid Reflectin Protein Impairs Tight Junction and Polarity in MDCK Cells

HU Biru#, SONG Junyi#*
(*College of Science, National University of Defense Technology, Changsha 410073, China*)

Abstract Cephalopods assemble periodic membrane architectures within iridocytes using reflectin proteins to generate tunable structural colors. However, the mechanisms underlying their intracellular trafficking, spatial organization and functional execution remain poorly understood. Previous studies have demonstrated that RefA1 (reflectin A1) obtained via heterologous expression in *Escherichia coli* displays high affinity for phospholipid membranes, while RefA1 expressed in HEK-293T cells by transient transfection undergoes directional traf-

收稿日期: 2025-12-10 接受日期: 2026-06-22
国家自然科学基金(批准号: 32201136)和国防科技大学自主科研基金资助的课题
#共同第一作者
*通信作者。Tel: 0731-84501311, E-mail: songjunyi@nudt.edu.cn
Received: December 10, 2025 Accepted: June 22, 2026
This work was supported by the National Natural Science Foundation of China (Grant No.32201136) and the Innovation Research Foundation of National University of Defense Technology
#These authors contributed equally to this work
*Corresponding author. Tel: +86-731-84501311, E-mail: songjunyi@nudt.edu.cn

ficking along the microtubule cytoskeleton. Therefore, the MDCK cell line, which possesses vesicular transport capacity and cytoskeletal plasticity, was selected as the research platform in this study. A cell model stably expressing squid-derived reflectin RefA1 was established to investigate its intracellular trafficking behavior and impacts on cellular structures. Results showed that RefA1 failed to yield the anticipated microtubule-guided subplasmalemmal enrichment, yet drastically disrupted cellular morphology and polarity. Cells expressing RefA1 presented reduced cell area, disassembled tight junctions, and became trapped in a “proliferation-detachment” cycle, preventing the formation of an intact cell monolayer. Transcriptomic analysis revealed that RefA1 severely perturbed the molecular networks governing cell junction assembly and polarity establishment. Specifically, it repressed the expression of polarity-determining factors including *CLDN4*, *CDH1* and *PARD6B*, while upregulating contractility-regulatory genes such as *MYLK2* and *ROCK1*. Collectively, these findings reveal for the first time that reflectin proteins not only interact with cell membranes and the cytoskeleton, but also actively modulate the establishment of cell polarity. This work offers novel insights into the cellular basis of photonic structures in cephalopods, and provides new clues for protein-mediated cellular morphogenesis engineering and biomimetic material design.

Keywords reflectin; MDCK cells; cell polarity; tight junction; transcriptome analysis

头足纲动物(如鱿鱼、章鱼、乌贼)因其卓越的动态变色能力而备受关注[1-3]。这种能力部分源于其皮肤中虹细胞(iridocytes)所产生的结构色——通过细胞内周期性排列的膜结合片层(即布拉格片层)实现光的选择性反射与干涉[4-8]。这一独特的生物光学结构, 为新型动态结构色体系与多光谱材料的设计提供了重要仿生学启示[9-11]。与以往认为虹细胞为静态光学元件的观点不同, 研究发现枪鱿科[如皮氏枪乌贼(*Doryteuthis pealeii*, *D. pealeii*)、加州笔管鱿鱼(*Doryteuthis opalescens*)等]虹细胞的反射状态可由神经递质乙酰胆碱可逆调控, 表明其具备动态光学响应能力[12-14]。

反射作用的分子基础在于一类被称为反射素(reflectins)的特异性蛋白家族。Crookes等[15]于2004年首次在鱿鱼反射组织中鉴定出该家族。反射素具有已知天然蛋白质中最高的折射率(1.591±0.002)[5], 这与其独特的氨基酸组成密切相关: 该家族蛋白缺乏丙氨酸、异亮氨酸、亮氨酸、赖氨酸等常见氨基酸残基, 而70%以上序列由酪氨酸、甲硫氨酸、精氨酸、天冬酰胺、甘氨酸和天冬氨酸6种氨基酸残基构成, 其中芳香族与含硫氨基酸占比高达43.8%[15]。研究进一步揭示, 反射素的磷酸化与去磷酸化可动态调节其净电荷及分子间作用, 进而影响片层间距、厚度与折射率, 最终实现对反射光谱的调控[16-17]。具体而言, 特定位点的磷酸化改变了反射蛋白的净电荷, 也扰乱了细胞内的Gibbs-Donnan平衡, 导致了片层间距、厚度和折射率的变化, 从而调控皮肤反射率[18-21]。值得关注的是, 氨基酸组成独特的反射素编码基因或源自与其共生的发光费氏弧菌(*Vibrio fischeri*)的水平基因转移; 一段编码八肽基序YMDMSGYQ的24 bp转座子序列在宿主基因组内复制, 最终演化出多基序的反射素家族[22]。尽管科学界逐渐建立起了对于其分子起源及其材料特性的认识, 但反射素蛋白与细胞膜协同组装、构建动态可调布拉格片层的关键细胞学机制仍未被阐明。

课题组前期的体外研究表明, 反射素蛋白[以反射素蛋白A1(reflectin A1, RefA1)为代表]对磷脂膜具有高亲和力与多价结合特性, 并能诱导囊泡聚集与膜融合, 提示其在膜结构重塑与组装中扮演主动角色[23]。在细胞层面, 于HEK-293T细胞中表达的RefA1可借助肌动蛋白锚定与微管运输, 定向富集于微管组织中心(microtubule organizing center, MTOC), 显示出与细胞骨架系统的密切互作[24]。这些特性暗示, 在天然虹细胞中, 反射素可能通过类似的细胞骨架驱动机制被运输至细胞膜周边区域并完成有序组装。然而, HEK-293T细胞的微管网络以核周MTOC为中心呈辐射状排列, 这限制了反射素向质膜下区域的主动运输, 难以模拟其在虹细胞中沿顶–基轴向的极性化分布。

为了克服上述模型系统的局限性, 并更直接地探究反射素在具有极性运输通道的细胞环境中的行为, 本研究选用Madin-Darby犬肾(Madin-Darby canine kidney, MDCK)上皮细胞系统作为实验平台[25-27]。MDCK细胞在建立顶–基极性后, 其

微管骨架会重排为纵向平行于细胞顶–基轴的阵列, 且微管负极朝向顶膜[28-29]。这种独特的细胞骨架构型为研究蛋白质从细胞内部向质膜下区域的定向运输提供了一个明确、可控的细胞模型。本文旨在利用该体系, 系统探究反射素蛋白RefA1在哺乳动物上皮细胞中的运输动力学及其对细胞结构与功能的影响。

本研究首先通过三质粒慢病毒系统构建了稳定表达RefA1的MDCK细胞系。出乎意料的是, 尽管未观察到RefA1沿微管向质膜下的预期富集, 但其持续性表达显著破坏了MDCK细胞的上皮形态、紧密连接完整性及顶–基极化能力。进一步的机制研究表明, RefA1的表达引起了包括密封蛋白4(claudin-4, *CLDN4*)、*CDH1*(cadherin 1)、*PARD6B*(partitioning defective 6 homolog beta)在内的多个关键极性决定因子显著下调表达, 并同时上调*MYLK2*(myosin light chain kinase 2)、*ROCK1*(Rho-associated, coiled-coil-containing protein kinase 1)等收缩调控基因的表达, 从而干扰了细胞紧密连接与极性建立的分子基础。上述结果首次证实, 反射素蛋白不只是具备特定折射率的生物光学元件, 还可作为调控因子主动干预细胞极性调控与细胞连接过程。本工作不仅拓展了对反射素蛋白细胞功能的认识, 也为理解头足纲动物虹细胞中独特光学结构自组装的细胞学基础提供了新的视角和实验依据。

1 材料与方法

1.1 试剂和仪器

本研究使用的主要试剂和仪器包括: BugBuster蛋白提取裂解液(EMD Millipore公司)、DMSO(dimethyl sulfoxide, ThermoFisher Scientific公司)、胎牛血清(foetal bovine serum, FBS; Gibco公司)、DMEM(Dulbecco's modified Eagle's medium, Gibco公司)、Lipofectamine 3000(ThermoFisher Scientific公司)、NBL-2细胞完全培养基(武汉普诺赛生命科技有限公司)、含DAPI抗荧光淬灭封片剂(DAPI-Fluoromount, 上海碧云天生物技术股份有限公司)、共聚焦显微镜(型号: Leica TCS SP8, Leica公司)。

1.2 反射素蛋白的表达与纯化

来自*D. pealeii*的RefA1的详细表达纯化流程见参考文献[23]。将表达质粒转化入Rosetta 2(DE3)大肠杆菌感受态细胞, 随后在LB(Luria-Bertani)培养基(含有50 μg/mL卡那霉素)中培养细胞(37 ℃、220 r/min)。通过添加1 mmol/L IPTG(isopropyl β-*D*-1-thiogalactopyranoside)诱导RefA1蛋白表达8 h。收集包涵体, 用BugBuster试剂进行溶解, 在含有6 mol/L盐酸胍、8 mol/L尿素的5%乙酸溶液中变性, 然后依次通过HiTrap SP XL阳离子交换树脂和反相色谱进行纯化。冻干后, 将RefA1蛋白重新溶解在超纯水中以获得水溶性储存液。通过SDS-PAGE验证RefA1蛋白纯度, 并检测280 nm波长处的吸光度(*D*)值以计算RefA1蛋白浓度。

1.3 蛋白质荧光标记与RNA混合孵育

蛋白质荧光染色: 向50 μmol/L RefA1蛋白溶液中加入5 mmol/L荧光素-5-马来酰亚胺(fluorescein-5-maleimide, 溶于DMSO)和1 mmol/L二硫苏糖醇(dithiothreitol, DTT)。反应混合物在4 ℃孵育过夜, 随后选用截留分子量小于20 kDa的超滤管进行超滤, 通过离心(4 500 ×*g*、4 ℃离心20 min)去除未结合的染料与游离试剂。将荧光素标记的RefA1与Cy5标记的*GFP*(green fluorescent protein) mRNA以不同浓度比例混合。由于RefA1带正电荷, 能自发地与带负电荷的mRNA结合, 混合数分钟内即可观察到明显的浑浊颗粒形成。取少量该悬浮液加入正常培养的HEK-293T细胞的培养基中(无需转染试剂)。4 h后, 在细胞内观察到蛋白的绿色荧光信号和mRNA的红色荧光信号, 表明二者已成功进入细胞。

1.4 重组pEGFP-C1载体的构建

针对哺乳动物表达系统对RefA1的编码序列进行密码子优化, 随后由生工生物工程(上海)股份有限公司合成带有RefA1编码序列的质粒并进行测序验证。为便于将RefA1编码序列克隆到pEGFP-C1载体中, 设计了含有*Eco*R I和*Bam*H I限制性内切酶酶切位点的正向和反向引物(F: 5′-GAA TTC TAT GAA TAG ATA TTT GAA TAG ACA-3′; R: 5′-GGA TCC ATA CAT ATG ATA ATC ATA ATA ATT T-3′)。然后, 利用限制性内切酶进行酶切, 结合DNA连接反应将修饰后的RefA1编码序列插入pEGFP-C1载体。

1.5 HEK-293T细胞系的培养与转染

将HEK-293T细胞于含10% FBS的DMEM中, 在37 ℃、5% CO_2的条件下培养。转染前一天, 将细胞以约30%汇合度接种到玻璃底培养皿(Cellvis公司)中, 贴壁生长24 h。使用Lipofectamine 3000按照试

剂说明书转染pEGFP-C1重组质粒, 随后将细胞继续培养16~24 h。

1.6 MDCK细胞系的培养

采用完全培养基培养MDCK(NBL-2)细胞, 细胞培养箱设置为37 ℃、5% CO_2。为获得极化的MDCK细胞, 在细胞汇合度达到100%后继续培养约72 h。对于MDCK_RefA1和MDCK_RefA1_GFP细胞系, 一旦观察到明显的细胞脱落, 即更换培养基: 首先用PBS轻轻洗涤细胞, 随后加入新鲜MDCK(NBL-2)培养基继续培养(37 ℃、5% CO_2)。

1.7 慢病毒生产与稳定细胞系构建

采用Lipofectamine 3000并按说明书操作, 将携带RefA1或RefA1_GFP编码序列的转移质粒pCDH-CMV-MCS-EF1-*mcherry*-T2A-Puro、包装质粒psPAX2与VSV-G包膜质粒pMD2.G以4:3:3的物质的量比(每10 cm培养皿总DNA为12 μg)进行共转染。在转染前18 h, 将约5×10^6个HEK-293T细胞接种至直径为10 cm的培养皿中; 当达到70%~80%汇合度时, 将培养基更换为6 mL Opti-MEM, 并加入DNA-脂质复合物。6 h后, 更换转染混合物为10 mL DMEM完全培养基(含10% FBS、1%青霉素/链霉素)。分别在转染后48 h和72 h收集含病毒上清, 混合, 通过0.45 μm PVDF滤膜(Millipore公司)过滤。将病毒沉淀轻轻重悬于100 μL预冷的PBS中, 分装并保存于–80 ℃。

1.8 转染与筛选

转染前18 h, 将靶细胞以30%~40%汇合度接种于12孔板。在加入病毒前立即添加聚凝胺(4 μg/mL)。12 h后更换接种液为完全培养基; 转染后48 h加入嘌呤霉素(1~2 μg/mL)。每48 h更换1次筛选培养基, 直至所有未转导的对照细胞被清除(通常6~8 d)。抗性细胞在早期传代时进行扩增和冻存。

1.9 单克隆细胞获取

为获得遗传背景均一的单克隆细胞系, 将上述筛选获得的细胞以极低密度(约每毫升10个细胞)接种至含嘌呤霉素培养基的96孔板中。在第10~14天可见单克隆细胞群, 于37 ℃用胰酶消化3 min, 然后将分散后的细胞重新置于37 ℃、5% CO_2培养箱中培养, 待汇合度达80%左右时, 收集细胞并冷冻保存于液氮中。

1.10 染色细胞的荧光成像

将培养在塑料培养皿(Cellvis公司)中的细胞用4%多聚甲醛室温固定30 min, 用含0.5% Triton X-100的PBS透化(室温处理10 min), 并用远红亲脂性细胞膜荧光探针(DiD)或微管蛋白示踪探针(Tubulin-Tracker)室温孵育30 min。PBS洗涤3次后, 采用DAPI-Fluoromount封片, 同步完成细胞核复染。在共聚焦显微镜上采集前述染色细胞的荧光图像, 并用ImageJ v1.52b软件进行图像处理[30]。

1.11 转录组获取与RNA-Seq分析

用Trizol试剂提取来自4个细胞组的12个样品的总RNA, 在液氮中速冻, 保存于干冰上, 并送至深圳华大基因股份有限公司进行RNA-Seq分析。使用Agilent 2100生物分析仪(Agilent公司)评估RNA质量(完整性、纯度、片段分布、浓度)。按照BGISEQ平台的标准方案制备测序文库, 步骤包括: 用oligo(dT)磁珠富集mRNA、mRNA片段化、第一链和第二链cDNA合成、cDNA末端修复、加A尾、接头连接及PCR扩增。合格的文库经环化形成DNA纳米球后, 在DNBSEQ平台上进行测序, 生成150 bp双末端读长的序列数据。后续的生物信息学分析通过深圳华大基因股份有限公司提供的Dr.Tom多组学整合分析平台完成。

1.12 统计分析

依托Dr.Tom多组学分析平台开展差异表达基因(differentially expressed genes, DEGs)分析, 采用平台内嵌DESeq2算法进行差异检验, 检验模型默认选用Wald检验; 所有基因的原始*P*值经Benjamini-Hochberg法进行错误发现率(false discovery rate, FDR)多重检验校正, 最终输出校正后*P*值(adjusted *P*-value)。细胞面积数据组间差异采用独立样本*t*检验进行统计学分析, 检验模式设置为双尾检验(two-tailed test), 方差齐性类型设定为类型3。

2 结果

2.1 RefA1的膜亲和力与细胞骨架引导的定向运输

课题组先前的研究表明, 反射素蛋白能够以高亲和力、多价结合的方式与磷脂膜相互作用, 并可诱导强烈的囊泡聚集及膜融合现象[23]。这些发现为理解虹细胞中反射素蛋白介导的膜结构重塑提供了初步的机制线索。然而, 人工脂质体模型在组成与结构复杂性方面与天然生物膜仍存在差距。因此, 为更贴近生理条件地探究反射素蛋白与生物膜的相互作用, 本研究利用HEK-293T细胞, 考察了重组表达(源于大肠杆菌)的RefA1在真核细胞质膜上的分

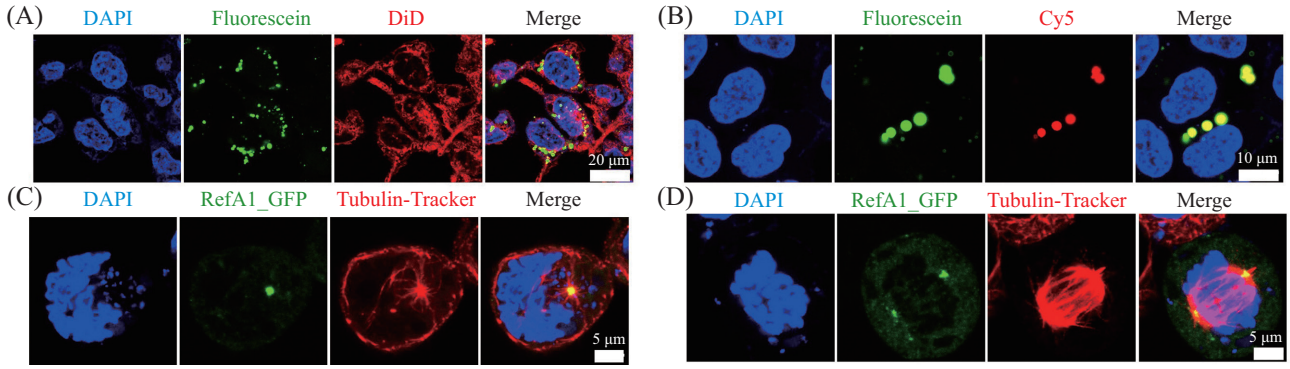

A: RefA1结合质膜及内吞作用。细胞核、RefA1和细胞膜分别用DAPI(蓝色)、fluorescein(绿色)和DiD(红色)染色。B: RefA1包载的mRNA通过内吞作用实现胞内递送。细胞核、RefA1和mRNA分别用DAPI(蓝色)、fluorescein(绿色)和Cy5(红色)染色。C、D: 胞内表达的RefA1表现出微管引导的定向运输及其在中心体周围的富集(图C: 分裂前期; 图D: 分裂后期)。细胞核和微管骨架分别用DAPI(蓝色)和Tubulin-Tracker(红色)染色, GFP标记的RefA1显示为绿色。

A: plasma membrane binding and endocytosis of RefA1. Nuclei, RefA1 and cell membranes were stained with DAPI (blue), fluorescein (green) and DiD (red), respectively. B: intracellular delivery of RefA1-encapsulated mRNA via endocytosis. Nuclei, RefA1 and mRNA were stained with DAPI (blue), fluorescein (green) and Cy5 (red), respectively. C,D: intracellularly expressed RefA1 exhibits microtubule-guided directional transport and accumulation at the centrosome (fig.C: prophase of cell division; fig.D: telophase of cell division). Cell nuclei and microtubule cytoskeletons were stained with DAPI (blue) and Tubulin-Tracker (red), respectively. GFP-tagged RefA1 is shown in green.

图1 HEK-293T细胞中RefA1膜亲和力及胞内定位的共聚焦显微镜分析

Fig.1 Confocal microscopic analysis of membrane affinity and subcellular localization of RefA1 in HEK-293T cells

布特征及其互作情况。

实验结果显示, 经绿色荧光标记的RefA1不仅能高效结合细胞质膜, 还可引发膜的局部曲率变化与内陷, 进而促进细胞发生内吞(图1A)。此外, RefA1能够有效包载Cy5标记的mRNA, 通过中和其表面负电荷, 实现该核酸分子向HEK-293T细胞的高效递送(图1B)。这些结果共同表明, RefA1具备较强的膜亲和性与膜重塑能力, 同时可作为带负电生物分子(如mRNA)进入细胞的递送载体。

膜亲和性仅是反射素蛋白发挥功能的理化基础, 其在特定亚细胞区域的空间富集对于维持虹细胞内布拉格片层的结构与功能同样至关重要。因此, 阐明反射素蛋白的定向运输与局部聚集机制, 是理解布拉格片层有序组装与动态调控的关键。之前的工作发现, 在HEK-293T细胞中表达的RefA1可借助细胞骨架系统, 通过肌动蛋白锚定与微管依赖的运输, 沿着微管网络负向运动, 富集于MTOC[24]。如图1C所示, 在细胞分裂前期, GFP标记的RefA1显著聚集于中心体周围, 该区域呈现辐射状微管分布。而在细胞分裂后期, 随着同源染色体分离, 中心粒逐渐分配至子细胞, 且RefA1仍保持在与分离中心粒相关的区域富集(图1D)。

这些现象支持如下假设: 在虹细胞中, 反射素蛋白的空间转运与组装很可能依赖于细胞骨架系统的精确调控。然而, HEK-293T细胞中MTOC主要位于核周区域, 该事实限制了RefA1向质膜下区域的靶向输送。因此我们推测, 采用具有纵向平行排列、顶–基极性化微管网络的细胞系统, 可能会为反射素蛋白向质膜下区域的定向运输提供更适宜的细胞骨架框架。

2.2 RefA1持续表达破坏MDCK细胞的紧密连接与细胞极性

经初步尝试, 发现使用脂质体瞬时转染难以在MDCK细胞中实现RefA1的高效表达。因此, 本研究采用三质粒慢病毒系统, 将RefA1编码序列整合至MDCK细胞基因组中, 以建立稳定表达RefA1的细胞系。通过提取基因组DNA并进行测序, 证实了外源基因的成功整合。

经过多代培养后, RefA1的表达显著改变了MDCK细胞的形态。实验设置4组细胞: MDCK(空白对照)、MDCK_Che_NS(表达荧光蛋白Cherry, 阴性对照)、MDCK_RefA1(稳定表达RefA1)及MDCK_RefA1_GFP(稳定表达GFP标记的RefA1)。如图2所示, 与对照组相比, 表达RefA1的细胞形态呈现高度不规则, 且细胞面积明显减小。具体而言, MDCK组(n=20)的平均细胞面积为(1 508.5±389.4) μm^2, MDCK_Che_NS组(n=20)为(1 236.4±255.1) μm^2; 而MDCK_RefA1(n=20)和MDCK_RefA1_GFP(n=20)组的平均细胞面积则分别降至(698.0±150.0) μm^{2}和(454.4±203.1) μm^2。值得指出

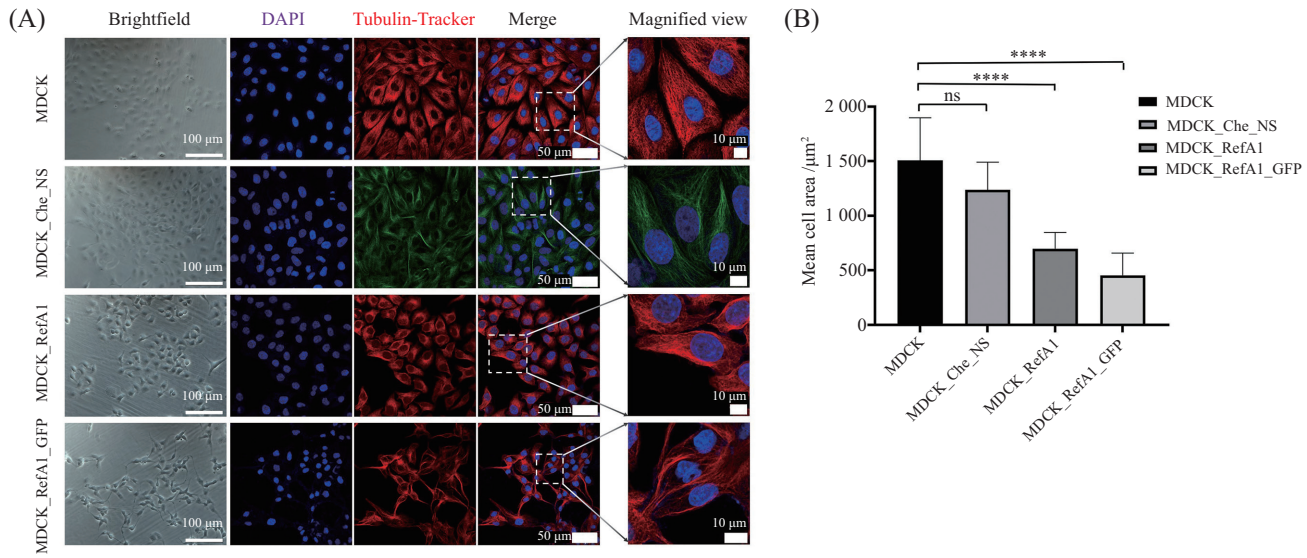

A: MDCK细胞形态。左列为相差显微图像。右侧3列为共聚焦显微镜成像结果: 细胞核用DAPI标记(蓝色)染色, 微管骨架用Tubulin-Tracker标记(MDCK_Che_NS组荧光为绿色, 其余3组荧光为红色)。B: 细胞平均面积的统计分析。误差棒=平均值±标准差。显著性通过*t*检验确定, $^{ns}P>0.05$, ****$P<0.000\ 1$, $n=20$。

A: morphology of MDCK cells. The left column shows phase contrast microscopic images. The three columns on the right display confocal laser scanning microscopy images: nuclei were stained with DAPI (blue), and microtubule cytoskeletons were labeled with Tubulin-Tracker (appearing green in the MDCK_Che_NS group and red in the other three groups). B: statistical analysis of mean cell area. Error bars represent $\bar{x}\pm s$. Statistical significance was determined by Student's *t*-test, $^{ns}P>0.05$, ****$P<0.000\ 1$, $n=20$.

图2 细胞形态与生长状态分析

Fig.2 Analysis of cellular morphology and growth status

的是, RefA1表达引起的细胞皱缩现象在HEK-293T细胞中曾有类似报道[31]。本研究发现, 在MDCK细胞中稳定表达RefA1可引发显著的细胞形态改变, 且该形态变化相较于HEK-293T细胞表现更为突出。

另一个值得关注的现象是, 对照组与表达RefA1的细胞在汇合行为上存在差异(图2A)。对照组MDCK和MDCK_Che_NS在接种后2~3 d内达到接近100%汇合度, 而MDCK_RefA1和MDCK_RefA1_GFP细胞持续保持分散状态, 无法形成连续的单细胞层。这一现象在长达数月的细胞培养以及多次实验中均获得重复验证, 排除了观测偏差的影响。后续转录组分析表明, RefA1的表达可破坏细胞的紧密连接结构, 从而阻碍细胞达到完全汇合, 并干扰后续的极化过程。

与对照组(MDCK和MDCK_Che_NS)细胞易于形成紧密汇合、结构完整的极化单层不同, 表达RefA1的细胞(MDCK_RefA1及MDCK_RefA1_GFP)始终无法达到完全汇合, 并随培养时间延长出现大规模脱落现象。

在初期, 这种脱落被推测为RefA1表达导致细胞活力下降所致。然而, 长期动态观察显示, 该现象实为RefA1表达赋予细胞的一种稳定表型。如图3所示, 培养14 d后, 对照组细胞已形成连接紧密、铺展均匀的连续单层; 相比之下, 大部分表达RefA1的细胞已从培养皿表面脱离, 悬浮于培养基中。经温和PBS洗涤后, 仅剩余少量稀疏贴壁的细胞。继续培养2 d, 这些存留的RefA1表达细胞迅速增殖, 证实其并未丧失活力与增殖能力, 但它们仍无法重建完整的上皮单层。

基于以上观察, RefA1表达细胞未能实现汇合并非由于增殖缺陷, 而是陷入了一个动态循环过程, 表现为"快速增殖→局部汇合→集体脱落→再增殖"的周期性行为。这一循环持续阻碍了稳定上皮单层及顶–基极性的建立。

2.3 RefA1表达引起细胞紧密连接及细胞极化损伤机制分析

为阐明RefA1表达引起细胞形态改变的分子机制, 我们进行了转录组测序分析。样品相关性分析显示, 各组内部生物学重复之间具有高度一致性(相关系数>0.980)。MDCK、MDCK_Che_NS与MDCK_RefA1_GFP 3组转录组数据呈现较高相关性(相关系数>0.890); 然而, MDCK_RefA1组与其余所有组别间的相关性均显著下降(图4A), 表明RefA1

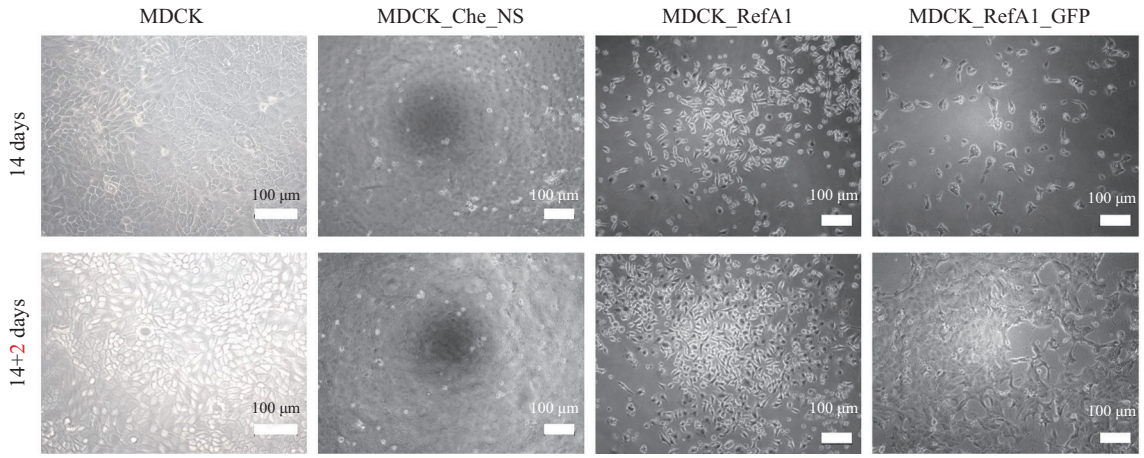

第一行显示传代后14 d的细胞状态; 第二行显示继续培养2 d(14 d+2 d)后的状态。

The first row shows cellular status at 14 days after passaging; the second row presents cell morphology after an additional 2 days (14 d+2 d) of culture.

图3 各组细胞生长状态分析

Fig.3 Analysis of cell growth status in different groups

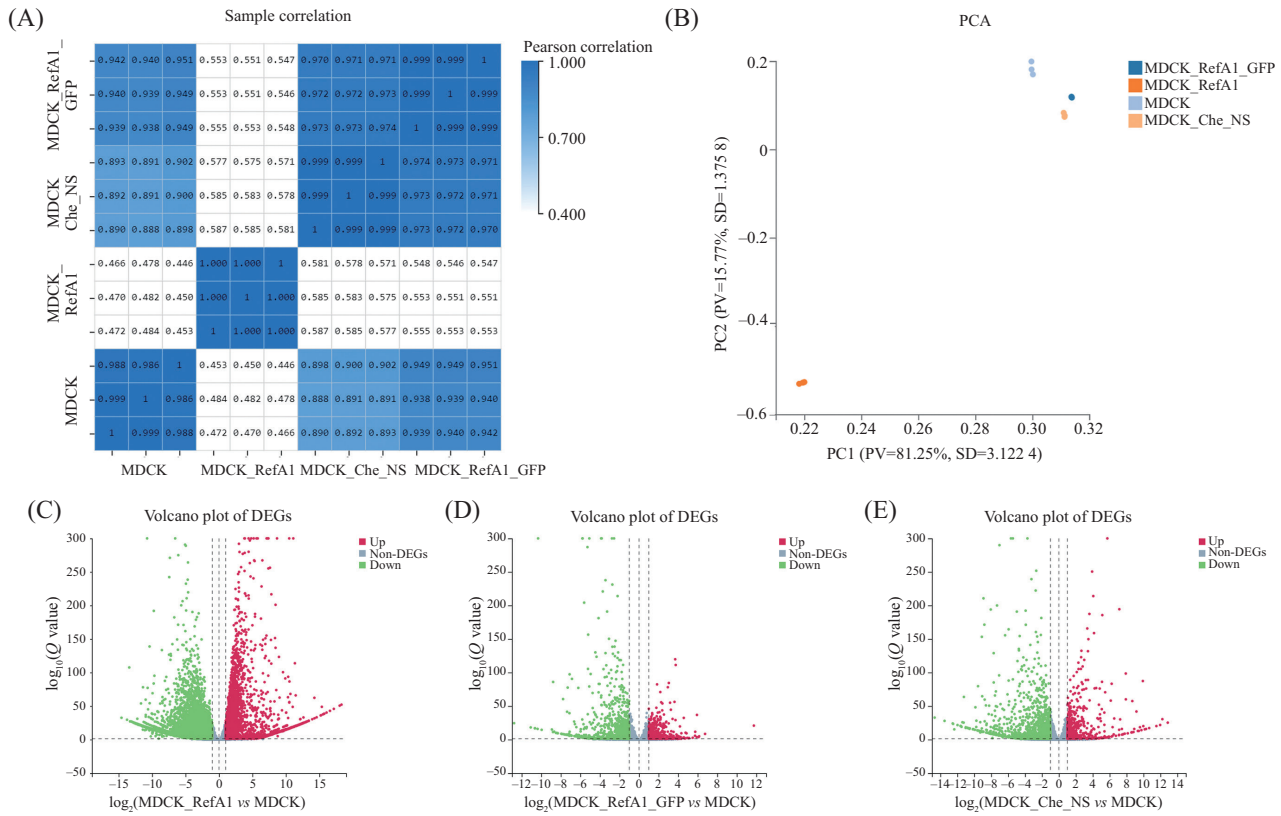

A: 样品相关性分析。B: PCA分析。C~E: 差异表达基因(DEGs)的火山图。横坐标代表基因表达的$\log_2$倍数变化, 纵坐标为$-\log_{10}(Q$值), 用于表征差异表达的统计学显著性。图中红点代表显著上调基因, 绿点代表显著下调基因, 灰色点为无显著差异基因。PV: 方差贡献率; SD: 标准差。

A: sample correlation analysis. B: PCA analysis. C-E: volcano plots of DEGs (differentially expressed genes). The horizontal axis represents $\log_2$(fold change) of gene expression, and the vertical axis denotes $-\log_{10}(Q$ value), which reflects the statistical significance of differential expression. Red dots indicate significantly up-regulated genes, green dots represent significantly down-regulated genes, and gray dots correspond to genes with no significant expression difference. PV: proportion of variance; SD: standard deviation.

图4 不同组细胞的基因表达分析

Fig.4 Analysis of gene expression of cells in different groups

表1 与紧密连接形成和极化受损相关的差异表达基因(MDCK_RefA1 *vs* MDCK)

Table 1 Differentially expressed genes associated with impaired tight junction formation and cell polarization (MDCK_RefA1 *vs* MDCK)

基因 Gene	log_2FC	功能 Function	参考文献 References
CLDN4 (claudin-4)	–7.61	Tight junction's primary transmembrane protein; its down-regulation will directly disrupt the epithelial barrier and weaken cell-cell adhesion	[32-33]
TJP2 (tight junction protein 2)	–1.87	Tight-junction cytoplasmic scaffolding protein; its reduced expression disrupts the claudin-occludin-actin interaction, precipitating junction disassembly	[34-35]
CDH1 (cadherin 1)	–11.36	Down-regulation of adherens junction core cadherins is a canonical EMT (epithelial-to-mesenchymal transition) signature; loss of adhesion renders cells prone to detachment	[36-37]
PARD6B (partitioning defective 6 homolog beta)	–6.97	An essential component in epithelial cell tight junction formation and maintenance of apico-basal polarity; its down-regulation will disrupt apical-basal polarity establishment, thereby preventing tight-junction maturation	[45-46]
PRKCI (protein kinase C iota)	–1.27	Localized at tight junctions, is indispensable for asymmetric junction formation and apico-basal polarity; its aberrant activity or mislocalization disrupts apicobasal polarity	[47]
CRB3 (Crumbs homolog 3)	–6.80	Apical polarity determinant; its down-regulation abrogates tight-junction assembly	[48-49]
MYLK2 (myosin light-chain kinase 2)	6.06	Phosphorylation of the myosin light chain drives actomyosin contraction; its up-regulation may disrupt junctional integrity and elevate intercellular permeability	[39-40]
ROCK1 (Rho-associated protein kinase 1)	1.05	Downstream kinase of RhoA; its hyperactivation promotes stress-fiber assembly and cellular contractility, leading to disruption of intercellular junctions	[41-43]
CFL1 (cofilin-1)	1.04	An actin-depolymerizing factor; dysregulation of its activity disrupts F-actin dynamics and compromises junctional stability	[44]

的稳定表达已引起细胞转录组的系统性重塑, 并可能影响关键细胞功能。

主成分分析(principal component analysis, PCA)进一步揭示了组间差异。MDCK、MDCK_RefA1、MDCK_RefA1_GFP、MDCK_Che_NS 4组样本各自的3个生物学重复数据点在图中紧密聚集, 表明各组内重复样本一致性高、实验重复性良好。值得注意的是, MDCK_RefA1组的数据点与其他组明显分离, 集中分布于左下象限, 而其余3组的数据点则共同位于右上区域(图4B)。这一空间分布模式再次直观表明, MDCK_RefA1细胞的基因表达谱与其他组存在本质性差异。

通过火山图展示组间DEGs(图4C)。结果显示, MDCK_RefA1组的基因表达情况与MDCK组相比差异最大, 共检测到3 172个上调基因和5 666个下调基因。相较之下, MDCK_Che_ NS组与MDCK_RefA1_GFP组的变化幅度较小, 分别有597个上调基因和1 328个下调基因, 以及475个上调基因和892个下调基因(图4C)。如此广泛的转录组改变, 充分说明RefA1的表达对细胞具有全局性影响。

在对转录组数据进行全面评估后, 进一步分析了DEGs列表, 以揭示MDCK_RefA1和MDCK_RefA1_GFP细胞系中紧密连接与细胞极性受损的分子机制。

首先, 针对MDCK_RefA1细胞中与紧密连接及极性形成相关的DEGs进行分析(表1)。结果显示, *CLDN4*的表达受到最显著抑制($log_2FC=-7.61$)[32-33], 其次为紧密连接蛋白2(tight junction protein 2, *TJP2*; 编码ZO-2; $log_2FC=-1.87$)[34-35], 黏附连接–连环蛋白轴同样严重受损——E-钙黏蛋白(E-cadherin, 由*CDH1*编码)表达水平急剧下降($log_2FC=-11.36$)[36-37]。

值得注意的是, 在细胞连接相关基因表达受抑的同时, 细胞收缩机制相关基因的表达却显著增强。肌动蛋白细胞骨架作为真核细胞基本结构与功能的执行者, 不仅为细胞形态发生与极性建立提供支架, 也参与细胞运动与分裂等过程[38]。尽管肌动蛋白本身的表达量未发生明显变化, 但其上游关键调控因子——*MYLK2*[39-40]与*ROCK1*[41-43]的表达均显著上调。这些变化共同导致连接周肌动蛋白环的结构紊乱, 从而在物理层面破坏细胞间连接的完整性[44]。

类似地, 对MDCK_RefA1_GFP细胞的转录组分析也揭示了一系列与细胞紧密连接及极性建立密切相关的基因表达下调(表2)。其

表2 与紧密连接形成和极化受损相关的差异表达基因(MDCK_RefA1_GFP *vs* MDCK)

Table 2 Differentially expressed genes associated with impaired tight junction formation and cell polarization (MDCK_RefA1_GFP *vs* MDCK)

基因 Gene	log_2FC	功能 Function	参考文献 References
CLDN1 (claudin-1)	−1.30	Core transmembrane proteins form the tight-junction strand; its down-regulation disrupts the strand, breaks epithelial barrier integrity and weakens cell-cell adhesion	[50-51]
CDH2 (cadherin 2)	−2.73	Cadherin family members mediate cell-cell adhesion; their abnormal down-regulation disrupts adhesive balance, destabilizing junctions and perturbing migration	[52-53]
CDC42EP3 (CDC42 effector protein 3)	−1.12	CDC42 effector; couples to CDC42 to steer cytoskeletal remodeling and set cell shape/polarity. Its down-regulation cripples CDC42 signaling, blocking polarity and directional migration	[54-55]
MYL9 (myosin light chain 9)	−1.21	Regulate myosin-II ATPase and contractility; at the rear, myosin-II contraction retracts the tail. Its down-regulation weakens this force, producing an extended “tailing edge” that fails to retract	[56-57]
TGM2 (transglutaminase 2)	−3.47	Orchestrate cell-matrix adhesion and ECM cross-linking, governing focal-adhesion turnover at the rear. Its down-regulation disrupts adhesion dynamics, impairing tail release and aggravating tail retention	[58-59]
TSPAN5 (tetraspanin 5)	−7.96	A tetraspanin family member that organizes functional membrane microdomains by clustering membrane proteins such as integrins and adhesion molecules, thereby regulating cell migration and signal transduction. Its down-regulation disrupts the assembly of cell-surface signaling complexes, impairs cell-matrix adhesion and focal-adhesion turnover at the rear, and causes tail-release failure	[60-61]
FLNC (filamin-C)	−1.66	An actin-crosslinking protein predominantly expressed in cardiac striated muscle, select smooth muscle and myofibroblast cells; it bundles actin into a dynamic gel and stabilizes focal adhesions via integrin binding. Its down-regulation disrupts the tail’s cortical actin mesh, reduces mechanical strength, and impairs adhesion maturation/turnover, yielding a loose tail that stretches abnormally during attempted retraction	[62-63]

中, *CLDN1*($log_2FC=-1.30$)与*CDH2*(cadherin 2, $log_2FC=-2.73$)表达同时受到抑制[50-53]。细胞极化迁移的进程高度依赖于CDC42(cell division cycle 42)信号轴介导的细胞骨架重塑。*CDC42EP3*(CDC42 effector protein 3, $log_2FC=-1.12$)的表达水平显著降低[54-55]。同时, 肌球蛋白轻链9(myosin light chain 9, *MYL9*; $log_2FC=-1.21$)编码激活肌球蛋白II ATP酶活性的调节亚基, 其表达量下降也使得细胞后缘的收缩性回缩出现障碍[56-57]。

细胞尾部回缩不仅依赖于细胞骨架的主动收缩, 还涉及细胞外基质(extracellular matrix, ECM)与肌动蛋白皮层的动态重构。在此过程中, 表达受抑制最显著的基因包括转谷氨酰胺酶-2(transglutaminase 2, *TGM2*; $log_2FC=-3.47$)与四跨膜蛋白5(tetraspanin 5, *TSPAN5*; $log_2FC=-7.96$)[58-61]。此外, *FLNC*(filamin-C, $log_2FC=-1.66$)的表达水平也下降[62-63]。上述基因表达的协同改变, 可合理解释在共聚焦显微镜下观察到的表达RefA1(GFP标记)的细胞所呈现的显著“拖尾”表型(图2A)。

另一个值得注意的现象是, MDCK_RefA1 *vs* MDCK与MDCK_RefA1_GFP *vs* MDCK的DEGs中, 有超过1 000个DEGs是相同的。在这些重叠基因中, 超过740个表现出一致的表达变化方向(同为上调或下调)。如此高的重叠度表明, 这两个细胞系的转录组重塑机制具有显著相似性。鉴于MDCK_RefA1_GFP组的DEGs数量较少, 推测串联的GFP标签可能部分遮蔽或干扰了RefA1的功能域, 进而削弱了其对全局基因表达的调控作用。

3 讨论

本研究在MDCK上皮细胞中成功建立了反射素蛋白RefA1的稳定表达体系, 并系统揭示了该蛋白对细胞结构与功能的深远影响。实验表明, RefA1的持续表达并未引导其沿极性微管系统定向富集于质膜下区域, 却意外引发了显著的表型改变: 细胞形态由规则上皮样转变为不规则小型化, 紧密连接完整性被破坏, 顶−基极性建立受阻, 且细胞呈现“增殖−汇合−脱落−再增殖”的周期性行为。

转录组分析进一步从分子层面阐释了RefA1表

达系统性瓦解上皮细胞的连接结构与极性程序的机制。对MDCK_RefA1细胞中紧密连接、细胞极性相关DEGs编码的蛋白进行分析可见, 紧密连接核心跨膜蛋白claudin-4表达受抑最为显著[32-33], 胞质斑块蛋白ZO-2表达下调次之。已有研究表明, 仅claudin-4缺失便可破坏细胞紧密连接[32-33]; 而ZO-2表达水平降低会阻碍claudin-occludin-肌动蛋白复合物形成, 加速连接结构解体[34-35]。黏附连接−连环蛋白通路同样发生严重损伤, E-钙黏蛋白编码基因*CDH1*表达水平大幅下降, 该基因下调往往与上皮−间质转化及细胞脱落密切相关[36-37]。此外, 细胞连接相关基因表达受到抑制时, 细胞收缩调控基因的转录水平却显著上调。肌动蛋白细胞骨架是真核细胞重要的结构与功能基础, 参与细胞形态建成、极性维持、运动及分裂等过程[38]。本研究中肌动蛋白表达未出现明显变化, 但其上游关键调控因子MYLK2与ROCK1均显著高表达。MYLK2可通过磷酸化肌球蛋白轻链, 提升肌动球蛋白的收缩张力[39-40]; ROCK1过度激活会促进应力纤维组装, 增强细胞向心收缩力[41-43]。此外, 肌动蛋白解聚因子CFL1(cofilin-1)表达异常, 会打破F-肌动蛋白动态平衡, 进一步削弱细胞连接稳定性[44]。

类似地, 对MDCK_RefA1_GFP细胞的转录组分析也揭示了一系列与细胞紧密连接及极性建立密切相关的基因表达下调。claudin-1(由*CLDN1*编码)与N-cadherin(由*CDH2*编码)作为紧密连接链与黏附连接链的核心跨膜支架蛋白, 其表达同时受到抑制, 将削弱细胞旁路屏障功能及侧向细胞间的黏附作用[50-53]。细胞极化迁移的进程高度依赖于CDC42信号轴介导的细胞骨架重塑。CDC42EP3的表达水平显著降低, 导致CDC42信号无法有效传递至其下游细胞骨架效应分子, 从而阻碍细胞前导缘的稳定形成[54-55]。同时, 细胞后缘的回缩也出现障碍: MYL9作为激活肌球蛋白II ATP酶活性的调节亚基, 其表达下调会减弱细胞后缘收缩力, 影响细胞尾部有效脱离[56-57]。细胞尾部回缩不仅依赖于细胞骨架的主动收缩, 还涉及ECM与肌动蛋白皮层的动态重构。在此过程中, 表达受抑制最显著的基因包括*TGM2*与*TSPAN5*。TGM2的表达下调降低了ECM交联效率, 延缓了黏着斑的更新; 而TSPAN5的缺失则破坏了富含整合素等黏附分子的膜微区结构, 损害了细胞基质黏附的动态调节[58-61]。这些变化共同导致细胞后缘与基底之间的黏附滞留时间延长, 使细胞尾部难以顺利脱离。此外, 肌动蛋白交联蛋白FLNC的表达水平也下降, 该蛋白通过连接整合素与收缩性细胞骨架维持细胞尾部结构的机械刚性, 其表达下调进一步削弱了细胞尾部脱离所需的力学支撑[62-63]。上述基因表达的协同改变, 可合理解释在共聚焦显微镜下观察到的GFP标记的RefA1表达细胞所呈现的显著“拖尾”表型。

由此可见, RefA1展现出多层次的细胞调控能力。该蛋白不仅具有膜亲和性与膜重塑活性, 还显示出与细胞骨架系统的密切互作——在HEK-293T细胞中依赖微管运输定向聚集于中心体区域。更为重要的是, 在MDCK细胞中, RefA1能引发广泛的转录组重编程, 影响细胞连接、极性建立、细胞骨架动力学及迁移相关的多条信号通路。这些发现共同说明, 反射素蛋白并非仅是具有高折射率的、受到被动调控的光学元件, 而是能够主动协调膜相互作用、细胞骨架运输与基因表达调控, 从而深刻影响细胞形态与功能的活性调控因子。

本工作首次将反射素蛋白的研究视角从材料光学特性拓展至细胞功能调控领域, 揭示了其在非天然细胞环境中调控细胞极性与紧密连接的新功能, 为理解头足纲动物虹细胞内布拉格片层的自组装与调控提供了新的细胞学思路。尽管在哺乳动物细胞中完全重构虹细胞样光学结构的直接目标尚未实现, 但所建立的细胞模型、发现的表型特性以及阐明的分子机制, 为后续探索蛋白质介导的亚细胞结构组装、仿生光学材料的细胞仿制, 乃至开发基于反射素的细胞工程工具奠定了重要的理论与实验基础。未来研究可进一步聚焦于优化蛋白递送与定位策略、解析RefA1与极性蛋白体系的相互作用网络, 或在具有更近似天然微环境的体外模型中尝试功能性的光学结构重建。

参考文献 (References)

[1] Mathger L M, Denton E J, Marshall N J, et al. Mechanisms and behavioural functions of structural coloration in cephalopods [J]. Journal of the Royal Society Interface, 2009, 6(S2): S149-S163.

[2] Williams T L, Senft S L, Yeo J, et al. Dynamic pigmentary and structural coloration within cephalopod chromatophore organs [J]. Nature Communications, 2019, 10(1): 1004.

[3] Mathger L M, Shashar N, Hanlon R T. Do cephalopods communicate using polarized light reflections from their skin? [J]. Journal of Experimental Biology, 2009, 212(Pt 14): 2133-2140.

[4] Bell G R, Mathger L M, Gao M, et al. Diffuse white structural coloration from multilayer reflectors in a squid [J]. Advanced

Materials, 2014, 26(25): 4352-4356.
[5] Kramer R M, Crookes-Goodson W J, Naik R R. The self-organizing properties of squid reflectin protein [J]. Nature Materials, 2007, 6(7): 533-538.
[6] Phan L, Walkup W G T, Ordinario D D, et al. Reconfigurable infrared camouflage coatings from a cephalopod protein [J]. Advanced Materials, 2013, 25(39): 5621-5625.
[7] Xu C Y, Stiubianu G T, Gorodetsky A A. Adaptive infrared-reflecting systems inspired by cephalopods [J]. Science, 2018, 359(6383): 1495-1500.
[8] Ordinario D D, Phan L, Walkup W G 4th, et al. Bulk protonic conductivity in a cephalopod structural protein [J]. Nature Chemistry, 2014, 6(7): 596-602.
[9] Bogdanov G, Strzelecka A A, Kaimal N, et al. Gradient refractive indices enable squid structural color and inspire multispectral materials [J]. Science, 2025, 388(6754): 1389-1395.
[10] Xu C Y. From nature's masters of camouflage to engineered optics: cephalopod-inspired materials and technologies [J]. Journal of Materials Chemistry C, 2025, 13(42): 21275-21301.
[11] Chatterjee A, Pratakshya P, Kwansa A L, et al. Squid skin cell-inspired refractive index mapping of cells, vesicles, and nanostructures [J]. ACS Biomaterials Science & Engineering, 2023, 9(2): 978-990.
[12] Mäthger L M, Collins T F, Lima P A. The role of muscarinic receptors and intracellular Ca^{2+} in the spectral reflectivity changes of squid iridophores [J]. Journal of Experimental Biology, 2004, 207(11): 1759-1769.
[13] Wardill T J, Gonzalez-Bellido P T, Crook R J, et al. Neural control of tuneable skin iridescence in squid [J]. Proceedings of the Royal Society B: Biological Sciences, 2012, 279(1745): 4243-4252.
[14] Hanlon R T, Cooper K M, Budelmann B U, et al. Physiological color change in squid iridophores [J]. Cell and Tissue Research, 1990, 259(1): 3-14.
[15] Crookes W J, Ding L L, Huang Q L, et al. Reflectins: the unusual proteins of squid reflective tissues [J]. Science, 2004, 303(5655): 235-238.
[16] Gordon R, Levenson R, Malady B, et al. Charge screening and hydrophobicity drive progressive assembly and liquid-liquid phase separation of reflectin protein [J]. Journal of Biological Chemistry, 2025, 301(3): 108277.
[17] Tobin C M, Gordon R, Tochikura S K, et al. Reversible and size-controlled assembly of reflectin proteins using a charged azobenzene photoswitch [J]. Chemical Science, 2024, 15(33): 13279-13289.
[18] Levenson R, Bracken C, Bush N, et al. Cyclable condensation and hierarchical assembly of metastable reflectin proteins, the drivers of tunable biophotonics [J]. Journal of Biological Chemistry, 2016, 291(8): 4058-4068.
[19] Demartini D G, Krogstad D V, Morse D E. Membrane invaginations facilitate reversible water flux driving tunable iridescence in a dynamic biophotonic system [J]. Proceedings of the National Academy of Sciences of the United States of America, 2013, 110(7): 2552-2556.
[20] Tao A R, Demartini D G, Izumi M, et al. The role of protein assembly in dynamically tunable bio-optical tissues [J]. Biomaterials, 2010, 31(5): 793-801.
[21] Izumi M, Sweeney A M, Demartini D, et al. Changes in reflectin protein phosphorylation are associated with dynamic iridescence in squid [J]. Journal of the Royal Society Interface, 2010, 7(44): 549-560.
[22] Guan Z, Cai T T, Liu Z M, et al. Origin of the reflectin gene and hierarchical assembly of its protein [J]. Current Biology, 2017, 27(18): 2833-2842,e6.
[23] Song J Y, Levenson R, Santos J, et al. Reflectin proteins bind and reorganize synthetic phospholipid vesicles [J]. Langmuir, 2020, 36(10): 2673-2682.
[24] Song J Y, Liu C Y, Li B S, et al. Tunable cellular localization and extensive cytoskeleton-interplay of reflectins [J]. Frontiers in Cell and Developmental Biology, 2022, 10: 862011.
[25] Zhang Y. Polyisocyanide hydrogels for modulating epithelial morphogenesis [D]. Nijmegen: Radboud Universiteit Nijmegen, 2021.
[26] Bre M, Pepperkok R, Hill A, et al. Regulation of microtubule dynamics and nucleation during polarization in MDCK II cells [J]. The Journal of Cell Biology, 1990, 111(6): 3013-3021.
[27] Green K J, Getsios S, Troyanovsky S, et al. Intercellular junction assembly, dynamics, and homeostasis [J]. Cold Spring Harbor Perspectives in Biology, 2009, 2(2): a000125.
[28] Martin-Belmonte F, Mostov K. Regulation of cell polarity during epithelial morphogenesis [J]. Current Opinion in Cell Biology, 2008, 20(2): 227-234.
[29] Jaulin F, Kreitzer G. KIF17 stabilizes microtubules and contributes to epithelial morphogenesis by acting at MT plus ends with EB1 and APC [J]. The Journal of Cell Biology, 2010, 190(3): 443-460.
[30] Schindelin J, Arganda-Carreras I, Frise E, et al. Fiji: an open-source platform for biological-image analysis [J]. Nature Methods, 2012, 9(7): 676-682.
[31] Chatterjee A, Cerna Sanchez J A, Yamauchi T, et al. Cephalopod-inspired optical engineering of human cells [J]. Nature Communications, 2020, 11(1): 2708.
[32] Van Itallie C M, Anderson J M. Claudin interactions in and out of the tight junction [J]. Tissue Barriers, 2014, 1(3): e25247.
[33] Van Itallie C M, Anderson J M. Claudins and epithelial paracellular transport [J]. Annual Review of Physiology, 2006, 68(1): 403-429.
[34] Traweger A, Toepfer S, Wagner R N, et al. Beyond cell-cell adhesion: emerging roles of the tight junction scaffold ZO-2 [J]. Tissue Barriers, 2013, 1(2): e25039.
[35] Traweger A, Fuchs R, Krizbai I A, et al. The tight junction protein ZO-2 localizes to the nucleus and interacts with the heterogeneous nuclear ribonucleoprotein scaffold attachment factor-B [J]. Journal of Biological Chemistry, 2003, 278(4): 2692-2700.
[36] Takeichi M. Cadherin cell adhesion receptors as a morphogenetic regulator [J]. Science, 1991, 251(5000): 1451-1455.
[37] Tan E J, Kahata K, Idås O, et al. The high mobility group A2 protein epigenetically silences the Cdh1 gene during epithelial-to-mesenchymal transition [J]. Nucleic Acids Research, 2015, 43(1): 162-178.
[38] Hall A. Rho GTPases and the actin cytoskeleton [J]. Science, 1998, 279(5350): 509-514.
[39] Garcia J, Lazar V, Gilbert-Mcclain L I, et al. Myosin light chain kinase in endothelium: molecular cloning and regulation [J].

American Journal of Respiratory Cell and Molecular Biology, 1997, 16(5): 489-494.

[40] Graham W V, He W Q, Marchiando A M, et al. Intracellular MLCK1 diversion reverses barrier loss to restore mucosal homeostasis [J]. Nature Medicine, 2019, 25(4): 690-700.

[41] Brown J. Investigating the actin cytoskeleton in cancer [D]. Glasgow: University of Glasgow, 2016.

[42] Riento K, Ridley A J. Rocks: multifunctional kinases in cell behaviour [J]. Nature Reviews Molecular Cell Biology, 2003, 4(6): 446-456.

[43] Daley W P, Gervais E M, Centanni S W, et al. ROCK1-directed basement membrane positioning coordinates epithelial tissue polarity [J]. Development, 2012, 139(2): 411-422.

[44] Bamburg J R. Proteins of the ADF/cofilin family: essential regulators of actin dynamics [J]. Annual Review of Cell and Developmental Biology, 1999, 15(1): 185-230.

[45] Macara I G. Par proteins: partners in polarization [J]. Current Biology, 2004, 14(4): R160-R162.

[46] Cunliffe H E, Jiang Y, Fornace K M, et al. PAR6B is required for tight junction formation and activated PKCζ localization in breast cancer [J]. American Journal of Cancer Research, 2012, 2(5): 478.

[47] Suzuki A, Hirata M, Kamimura K, et al. aPKC acts upstream of PAR-1b in both the establishment and maintenance of mammalian epithelial polarity [J]. Current Biology, 2004, 14(16): 1425-1435.

[48] Lemmers C, Michel D, Lane-Guermonprez L, et al. CRB3 binds directly to Par6 and regulates the morphogenesis of the tight junctions in mammalian epithelial cells [J]. Molecular Biology of the Cell, 2004, 15(3): 1324-1333.

[49] Roh M H, Fan S L, Liu C J, et al. The Crumbs3-Pals1 complex participates in the establishment of polarity in mammalian epithelial cells [J]. Journal of Cell Science, 2003, 116(14): 2895-2906.

[50] Furuse M, Hata M, Furuse K, et al. Claudin-based tight junctions are crucial for the mammalian epidermal barrier: a lesson from claudin-1-deficient mice [J]. The Journal of Cell Biology, 2002, 156(6): 1099-1111.

[51] Tsukita S, Furuse M. The structure and function of claudins, cell adhesion molecules at tight junctions [J]. Annals of the New York Academy of Sciences, 2000, 915(1): 129-135.

[52] Wheelock M J, Johnson K R. Cadherins as modulators of cellular phenotype [J]. Annual Review of Cell and Developmental Biology, 2003, 19(1): 207-235.

[53] Cavallaro U, Christofori G. Cell adhesion and signalling by cadherins and Ig-CAMs in cancer [J]. Nature Reviews Cancer, 2004, 4(2): 118-132.

[54] Farrugia A J, Calvo F. The Borg family of Cdc42 effector proteins Cdc42EP1-5 [J]. Biochemical Society Transactions, 2016, 44(6): 1709-1716.

[55] Pichaud F, Walther R F, Nunes De Almeida F. Regulation of Cdc42 and its effectors in epithelial morphogenesis [J]. Journal of Cell Science, 2019, 132(10): jcs217869.

[56] Totsukawa G, Wu Y, Sasaki Y, et al. Distinct roles of MLCK and ROCK in the regulation of membrane protrusions and focal adhesion dynamics during cell migration of fibroblasts [J]. The Journal of Cell Biology, 2004, 164(3): 427-439.

[57] Betapudi V, Licate L S, Egelhoff T T. Distinct roles of nonmuscle myosin II isoforms in the regulation of MDA-MB-231 breast cancer cell spreading and migration [J]. Cancer Research, 2006, 66(9): 4725-4733.

[58] Fesus L, Piacentini M. Transglutaminase 2: an enigmatic enzyme with diverse functions [J]. Trends in Biochemical Sciences, 2002, 27(10): 534-539.

[59] Akimov S S, Krylov D, Fleischman L F, et al. Tissue transglutaminase is an integrin-binding adhesion coreceptor for fibronectin [J]. The Journal of Cell Biology, 2000, 148(4): 825-838.

[60] Hemler M E. Tetraspanin proteins mediate cellular penetration, invasion, and fusion events and define a novel type of membrane microdomain [J]. Annual Review of Cell and Developmental Biology, 2003, 19(1): 397-422.

[61] Yáñez-Mó M, Barreiro O, Gordon-Alonso M, et al. Tetraspanin-enriched microdomains: a functional unit in cell plasma membranes [J]. Trends in Cell Biology, 2009, 19(9): 434-446.

[62] Zhou A X, Hartwig J H, Akyürek L M. Filamins in cell signaling, transcription and organ development [J]. Trends in Cell Biology, 2010, 20(2): 113-123.

[63] Kajita M, Sugimura K, Ohoka A, et al. Filamin acts as a key regulator in epithelial defence against transformed cells [J]. Nature Communications, 2014, 5(1): 4428.